A γ-secretase inhibitor and quinacrine reduce prions and prevent dendritic degeneration in murine brains

Patricia Spilman*, Pierre Lessard†, Mamta Sattavat*, Clarissa Bush*, Thomas Tousseyn*‡, Eric J. Huang*, Kurt Giles†§, Todd Golde¶, Pritam Das¶, Abdul Fauq¶, Stanley B. Prusiner†§‖, and Stephen J. DeArmond*†‖

Departments of *Pathology and §Neurology and †Institute for Neurodegenerative Disease, University of California, San Francisco, CA 94143; ‡Laboratory for Neuronal Cell Biology and Gene Transfer, Department for Human Genetics, Flanders Institute for Biotechnology 4, Katholieke Universiteit Leuven, 3000 Leuven, Belgium; and ¶Department of Neuroscience, Mayo Clinic College of Medicine, Jacksonville, FL 32224

Contributed by Stanley B. Prusiner, University of California, San Francisco, CA, April 15, 2008 (sent for review December 7, 2007)

In prion-infected mice, both the Notch-1 intracellular domain transcription factor (NICD) and the disease-causing prion protein (PrP^{Sc}) increase in the brain preceding dendritic atrophy and loss. Because the drug LY411575 inhibits the γ-secretase-catalyzed cleavage of Notch-1 that produces NICD, we asked whether this γ-secretase inhibitor (GSI) might prevent dendritic degeneration in mice with scrapie. At 50 d postinoculation with Rocky Mountain Laboratory (RML) prions, mice were given GSI orally for 43–60 d. Because we did not expect GSI to produce a reduction of PrP^{Sc} levels in brain, we added quinacrine (Qa) to the treatment regimen. Qa inhibits PrP^{Sc} formation in cultured cells. The combination of GSI and Qa reduced PrP^{Sc} by ≈95% in the neocortex and hippocampus but only ≈50% in the thalamus at the site of prion inoculation. The GSI plus Qa combination prevented dendritic atrophy and loss, but GSI alone did not. Even though GSI reduced NICD levels to a greater extent than GSI plus Qa, it was unable to prevent dendritic degeneration. Whether a balance between NICD and dendrite growth-stimulating factors was achieved with GSI plus Qa but not GSI alone remains to be determined. Although the combination of GSI and Qa diminished PrP^{Sc} in the brains of RML-infected mice, GSI toxicity prevented us from being able to assess the effect the GSI plus Qa combination on incubation times. Whether less toxic GSIs can be used in place of LY411575 to prolong survival remains to be determined.

Creutzfeldt–Jakob disease | neuropathology | prion disease | therapy | scrapie

Prion diseases are rapidly progressive, invariably fatal neurodegenerative disorders caused by the accumulation of PrP^{Sc}, the pathogenic isoform of the prion protein (1–6). A wealth of evidence argues that PrP^{Sc} is the sole component of the infectious prion particle. To date, no pharmacologic intervention has effectively cleared PrP^{Sc} from the brain or prevented neurodegeneration in humans with Creutzfeldt–Jakob disease (CJD) or experimental animals with scrapie (7–9). By the time most patients are diagnosed with prion disease, pronounced neurological deficits are present. CJD is a rapidly progressive illness that generally leads to death in 3–6 months. At autopsy, synaptic degeneration and nerve cell death and widespread astrocytic gliosis are found.

In prion-infected rodents, neurodegeneration begins with the accumulation of PrP^{Sc} in neuronal membranes, followed by dendritic atrophy and loss and finally nerve cell death (1, 4, 10). During studies on the pathogenesis of experimental scrapie in mice, we found that the release of the Notch-1 intracellular domain transcription factor (NICD) preceded early dendritic atrophy in scrapie-infected mice (4). Notch-1 activation requires multiple enzymatic cleavage steps culminating in the γ-secretase-mediated release of NICD (11–13).

Translocation of NICD to neuronal nuclei stimulates expression of genes whose gene products, such as the Hes family of proteins, inhibit expression of genes that maintain dendrites and axons, particularly during CNS development (14, 15). To test the hypothesis that PrP^{Sc}-related activation of Notch-1 repressor signaling pathways is a major cause of early dendritic atrophy, we treated prion-infected mice with the γ-secretase inhibitor (GSI) LY411575 (16, 17).

Toward enhancing the efficacy of the GSI, we added the drug quinacrine (Qa), which inhibits PrP^{Sc} formation in cultured cells (18, 19). Although Qa alone modestly lowered PrP^{Sc} levels *in vivo*, it failed to prolong incubation times in prion-infected, wild-type mice (20, 21). Subsequent studies revealed that the levels of Qa in the brains of these animals were too low to be therapeutic (K.G. and S.B.P., unpublished data). During studies of Qa metabolism in mice, we found that Qa efflux from the brain is controlled by multidrug-resistant (MDR) proteins, members of the P-glycoprotein ATP binding cassette transporters (22). Disappointingly, MDR-deficient mice accumulate high levels of Qa in their brains but fail to show prolonged survival after prion inoculation (K.G. and S.B.P., unpublished data).

When GSI and Qa were administered together, they reduced PrP^{Sc} levels 50% in the thalamus around the site of inoculation and 95% in the cortex and hippocampus. Long axonal projections connect the thalamus to the cerebral cortex. GSI appeared to decrease axonal transport of PrP^{Sc}, halting the spread of prion disease from one brain region to another. Qa alone seemed to diminish dendritic atrophy and loss. Although GSI and Qa suppressed the levels of both PrP^{Sc} and NICD and prevented dendritic atrophy, this combination therapy did not prolong the lives of prion-inoculated mice compared with uninoculated controls due to GSI toxicity. Whether other less toxic GSIs can be used in place of LY411575 to prolong survival remains to be determined.

Results

Experimental Design. Wild-type, male CD1 mice were inoculated at 7 weeks of age in the right thalamus with 30 μl of a 10% brain homogenate containing 10^6 ID_{50} units of Rocky Mountain Laboratory (RML) prions (6). Age-matched controls were inoculated with the same volume of a 10% brain homogenate from normal, uninfected CD1 mice. RML-inoculated CD1 mice showed clinical signs of disease beginning at ≈120 d postinoculation (dpi) [supporting information (SI) Fig. S1]. Treatment with GSI alone, Qa alone, or a combination of GSI plus Qa was begun at 50 dpi when PrP^{Sc} accumulation was well established in the thalamus and just beginning in the neocortex and hippocampus (6). Both drugs were given ad libitum by the oral route mixed

Author contributions: P.S., E.J.H., S.B.P., and S.J.D. designed research; P.S., P.L., C.B., and K.G. performed research; T.G., P.D., and A.F. contributed new reagents/analytic tools; M.S. and T.T. analyzed data; and P.S., S.B.P., and S.J.D. wrote the paper.

The authors declare no conflict of interest.

‖To whom correspondence may be addressed. E-mail: stephen.dearmond@ucsf.edu or stanley@ind.ucsf.edu .

This article contains supporting information online at www.pnas.org/cgi/content/full/0803671105/DCSupplemental.

© 2008 by The National Academy of Sciences of the USA

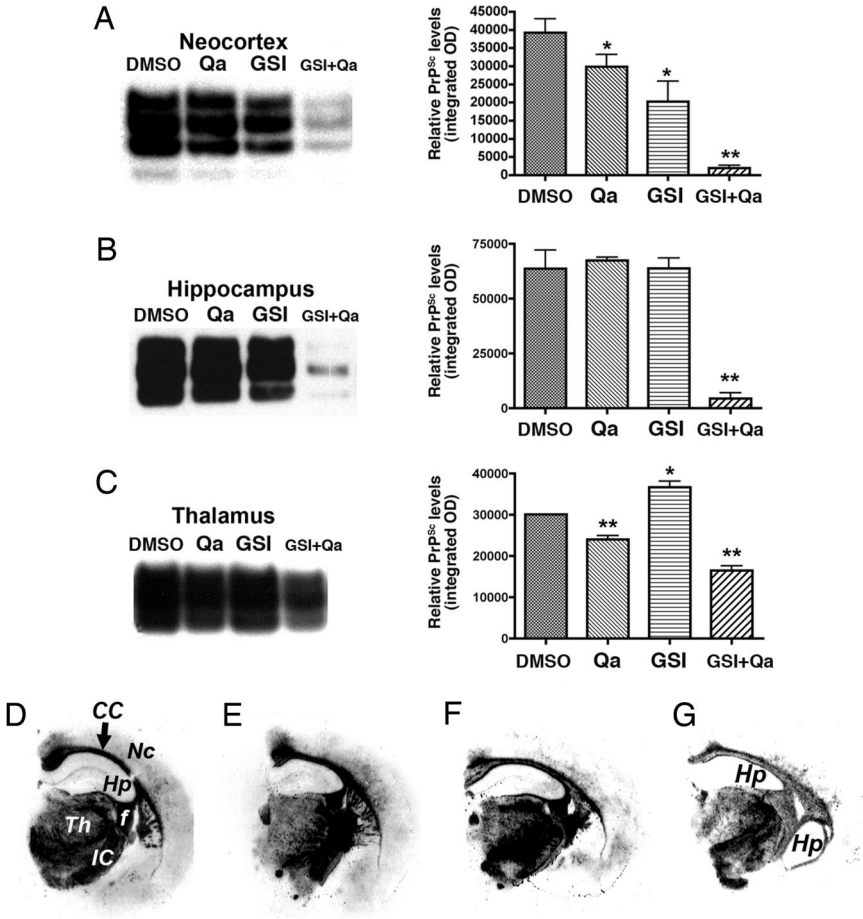

Fig. 1. Combined GSI and Qa therapy reduced PrP^{Sc} by 95% in the neocortex and hippocampus and by 50% in the thalamus from prion-infected mice. (*A–C*) Western immunoblots of protease-resistant PrP^{Sc} in the neocortex (*A*), hippocampus (*B*), and thalamus (*C*) are shown from mice given chocolate drink with 0.007% DMSO containing no drug for 60 d (DMSO), Qa alone for 60 d (Qa), GSI alone for 56 d (GSI), and GSI plus Qa for 43 d. Film exposure time was adjusted to reveal PrP^{Sc} in the neocortex and hippocampus from mice treated with GSI plus Qa. Adjacent bar graphs show densitometry estimates of the relative PrP^{Sc} levels in the respective Western blots (integrated optical density units per milligram of total protein). Means and standard deviations are shown. Student's *t* test probabilities ($n = 3$ mice each): *, $P \leq 0.05$; **, $P \leq 0.01$. (*D–G*) Protease-resistant PrP^{Sc} immunostained in histoblots of coronal sections of the cerebral hemisphere through the dorsal hippocampus where it overlies the thalamus are shown. Samples were taken from RML-infected mice at 100 dpi given chocolate drink with DMSO only (*D*), Qa only (*E*), GSI only (*F*), and combined GSI plus Qa (*G*). CC, corpus callosum; f, fimbria of fornix; Hp, hippocampus; IC, internal capsule; Nc, neocortex; Th, thalamus.

in a chocolate drink containing pulverized lab chow to mask the bitter taste of Qa. The (*S*)-enantiomer of LY411575 was dissolved in DMSO to ensure uniform mixing in the chocolate drink; the final concentration of DMSO was ≈0.007% in all drink preparations unless specified. Although 100-fold higher concentrations of DMSO were reported to reduce the rate of PrP^{Sc} accumulation in the brain (23), we found no effect on PrP^{Sc} levels in prion-infected mice fed the chocolate drink with 0.007% DMSO compared with those fed the chocolate drink without DMSO (data not shown). The doses of GSI chosen for this study were 5 or 10 $mg{\cdot}kg^{-1}{\cdot}d^{-1}$; the Qa dose was 40 $mg{\cdot}kg^{-1}{\cdot}d^{-1}$ (24). Prion-infected, control mice fed a diet with DMSO but lacking either GSI or Qa were designated "DMSO."

All currently available GSIs are accompanied by adverse side effects in mice, including hunched posture, hair loss, and marked (≈10 g) weight loss (25). GSI at a concentration of 10 $mg{\cdot}kg^{-1}{\cdot}d^{-1}$ combined with 40 $mg{\cdot}kg^{-1}{\cdot}d^{-1}$ Qa produced severe side effects by 13 d of treatment in both uninfected control and RML-infected mice, which required euthanasia (Fig. S1). In RML-infected mice and uninfected control mice given 5 $mg{\cdot}kg^{-1}{\cdot}d^{-1}$ GSI combined with 40 $mg{\cdot}kg^{-1}{\cdot}d^{-1}$ Qa, six of nine mice survived 43 d of treatment. At this time point, all six surviving mice were killed; notably, five mice were free of signs of GSI toxicity. Uninfected control mice given 5 or 10 $mg{\cdot}kg^{-1}{\cdot}d^{-1}$ GSI alone developed the same side effects as RML-infected mice, indicating that GSI, not prion disease, was responsible for the observed toxicity. Given the extreme adverse effects of 10 $mg{\cdot}kg^{-1}{\cdot}d^{-1}$ GSI, we used only mice given 5 $mg{\cdot}kg^{-1}{\cdot}d^{-1}$ GSI alone or in combination with 40 $mg{\cdot}kg^{-1}{\cdot}d^{-1}$ Qa for the analysis reported here.

GSI and Qa Reduce PrP^{Sc}. GSI plus Qa for 43 d (93 dpi) decreased the levels of PrP^{Sc} in the cortex and hippocampus of RML-infected mice by ≈95% compared with untreated, control DMSO mice that were inoculated intracerebrally with RML prions, fed chocolate drink with DMSO, and killed 110 dpi (Fig. 1 *A*, *B*, *D*, and *G*). In addition to these infected control DMSO mice, we killed some at 93 dpi as controls for the treated group. When these control DMSO mice were compared with the treated group, a similar 95% reduction of PrP^{Sc} was found in the treated mice (Fig. S2).

In the thalamus, where prion replication was initiated, GSI plus Qa treatment reduced PrP^{Sc} levels by only ≈50% (Fig. 1 *C*, *D*, and *G*). In comparison, Qa alone reduced PrP^{Sc} by only ≈20%

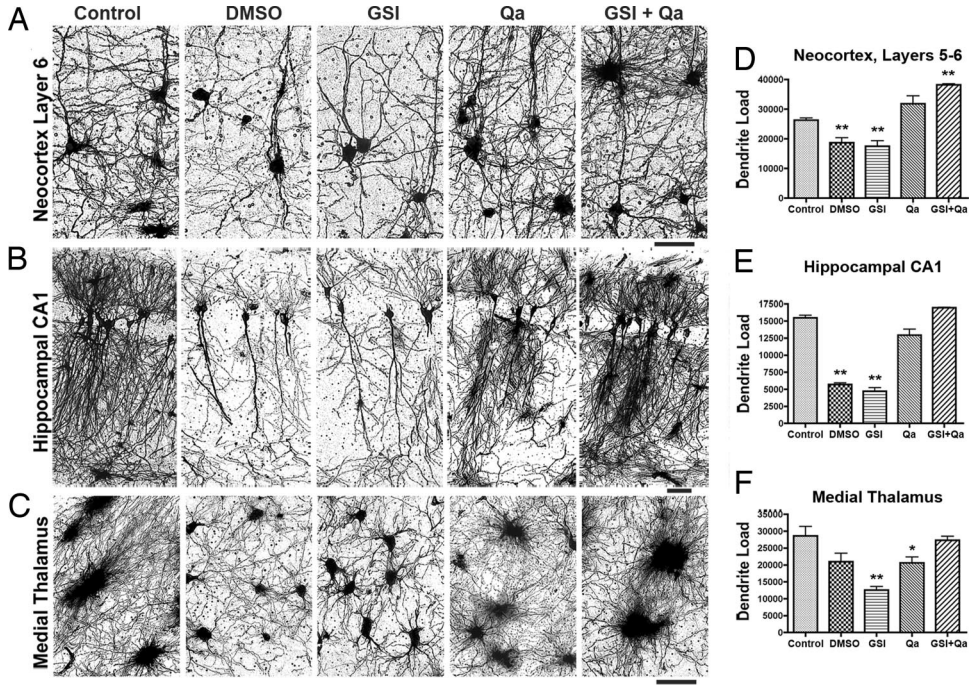

Fig. 2. Dual GSI plus Qa therapy prevented dendritic degeneration more effectively than GSI or Qa alone. (*A–C*) Golgi silver staining of dendrites in layer 6 of the cortex (*A*), the hippocampus CA1 region (*B*), and the medial nuclei of the thalamus (*C*) shows severe dendrite loss in infected DMSO mice and prevention of loss with GSI plus Qa treatment. (*D–F*) Measurements of dendrite loads in each of the three brain regions as a function of treatment are shown. Note the microscopic field used to measure dendrite loads in the cortex spanned cortical layers 5 and 6, whereas the micrographs in *A* show cortex layer 6 only. Student's *t* test probabilities ($n = 3$ mice each): *, $P \leq 0.05$; **, $P \leq 0.01$. Scale bars represent 30 μm and apply to each image in the same row.

in the thalamus (Fig. 1 *C–E*) and cortex (Fig. 1 *A*, *D*, and *E*). GSI alone reduced PrP^{Sc} by ≈50% in the cortex (Fig. 1 *A*, *D*, and *F*) and unexpectedly increased PrP^{Sc} by ≈20% in the thalamus (Fig. 1 *C*, *D*, and *F*). In the hippocampus, GSI alone and Qa alone had no effect on PrP^{Sc} levels (Fig. 1 *B* and *D–F*). The reductions in PrP^{Sc} levels in the cortex and hippocampus with GSI plus Qa were greater than the sums of the reductions from treatments with either GSI or Qa alone, suggesting that the two drugs work synergistically to decrease PrP^{Sc}. Reductions in PrP^{Sc} levels were not due to diminished expression of PrP^{C} because PrP^{C} levels in the cortex were unchanged in uninfected controls given chocolate drink with or without DMSO and those treated with GSI, Qa, or GSI plus Qa (Fig. S3). The uninfected control mice were inoculated with brain homogenate from uninfected mice.

GSI and Qa Prevent Dendritic Degeneration. Among the earliest neurodegenerative changes in experimental scrapie are shortening of dendrites and decreased numbers of dendritic branches and spines (4, 10). To analyze quantitatively neurodegenerative changes in our treated mice, we estimated the "dendrite load," a measure of the area of a gray matter field occupied by Golgi silver-impregnated dendrites and nerve cell bodies. With GSI plus Qa treatment, dendrite loads were similar to those of uninfected controls or even increased (Fig. 2). As shown, degenerative changes in RML-infected, control DMSO mice were severe at 93 dpi (compare with Fig. 2 *A–C*) (4). Thus, the combination of GSI and Qa prevented dendritic atrophy and loss in both the cortex and hippocampus, consistent with ≈95% reductions of PrP^{Sc} in the same brain regions. In the thalamus, GSI plus Qa therapy reduced PrP^{Sc} levels by only ≈50% (Fig. 1*C*) yet preserved the dendrite load (Fig. 2 *C* and *F*).

NICD Levels and Dendritic Degeneration. On the basis of the finding that synaptosomal PrP^{Sc} accumulation is temporally associated with both increased nuclear NICD and degeneration of dendrites (4), we hypothesized that the accumulation of NICD causes dendritic atrophy and loss. Consistent with that hypothesis, RML-infected DMSO mice have low cortical dendrite loads and high NICD levels (Figs. 2*D* and 3*A*). Contrary to this hypothesis, low cortical dendrite loads and low NICD levels were found in RML-infected mice treated with GSI alone (Fig. 3). Plotting the cortical dendrite loads (Fig. 2*D*) as a function of cortical nuclear NICD levels (Fig. 3*B*) shows that the most severe loss of dendrites occurred at extreme NICD concentrations (Fig. 3*C*). The lowest NICD concentration was in prion-infected mice treated with GSI alone, and the highest in prion-infected, control DMSO mice. In contrast, intermediate levels of NICD in mice treated with either Qa alone or GSI plus Qa, which were near uninfected control levels, were associated with the preservation of dendrites (Fig. 3*C*).

GSI Toxicity Dependence on Dose and Duration of Exposure. The beneficial effects of combining GSI with Qa to treat prion disease were marred by severe, adverse drug reactions, leading to premature deaths: Treated, prion-infected mice died substantially sooner than untreated, prion-infected mice (Fig. S1*A*). Administration of 10 $mg \cdot kg^{-1} \cdot d^{-1}$ GSI plus Qa resulted in death after ≈13 d of treatment in both infected and uninfected mice. Lower doses of GSI alone or with Qa were tolerated for longer treatment durations, but all animals eventually had to be euthanized within ≈56 d of continuous treatment (Fig. S1). We attribute this toxicity mainly to the GSI, but Qa also seems to contribute to the adverse effects. Infected mice treated with 5 $mg \cdot kg^{-1} \cdot d^{-1}$ GSI alone survived longer than those given GSI plus Qa. Notably, Qa is known to affect hepatic, cardiac, and CNS function; jaundice, cardiomyopathy, slowing of electrical conduction in the heart, and seizures are among the known side effects (26, 27). The adverse side effects related to the GSI are likely in part due to inhibition of Notch-1 signaling, which encourages goblet cell differentiation in the gut and a shift

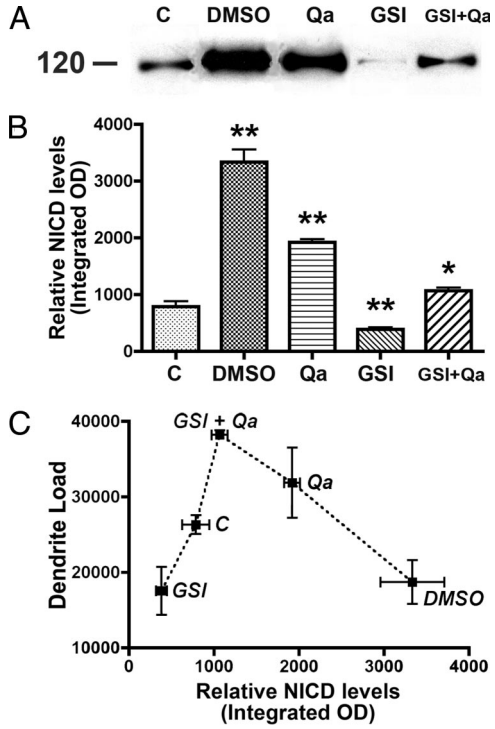

Fig. 3. The three treatments had significantly different effects on nuclear NICD levels in the cortex. (*A*) Western immunoblot analysis shows nuclear NICD levels from prion-infected mice after treatment with Qa alone, GSI alone, and GSI plus Qa. As controls, nuclear NICD levels in an uninfected mouse (control, C) and an untreated, prion-infected mouse (DMSO) are shown. (*B*) Quantification of relative nuclear NICD concentrations is given; numbers correspond to treatments described in *A*. Student's *t* test probabilities ($n = 3$ mice each): *, $P \leq 0.05$; **, $P \leq 0.01$. (*C*) NICD levels are dissociated from dendritic degeneration. Cortex dendrite load (see Fig. 2*D*) is graphed as a function of the nuclear NICD concentration shown in *B*.

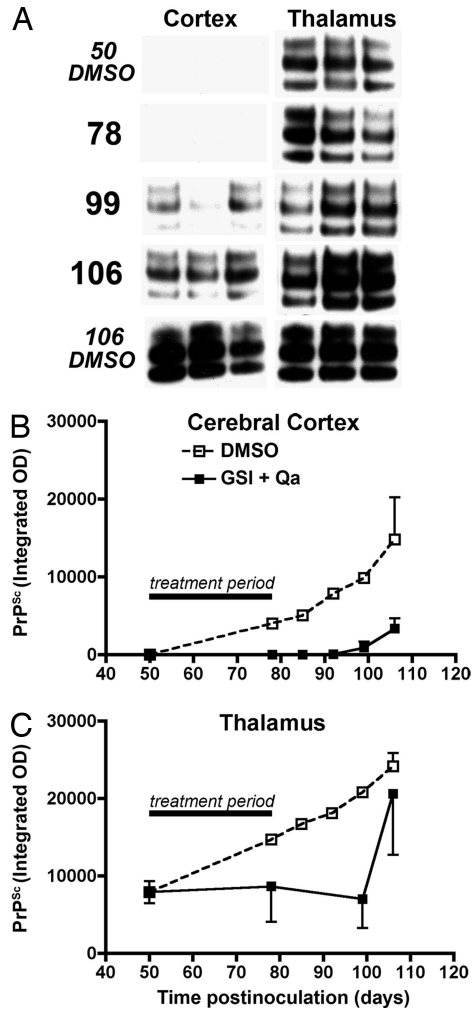

Fig. 4. After 28 d of treatment with GSI plus Qa, PrP^{Sc} levels remain low for 21 d after treatment is ceased. (*A*) Western immunoblots of PrP^{Sc} in the cortex and thalamus from three mice each at 50, 78, 99, and 106 dpi are shown (85 and 92 dpi; data not shown). (*B* and *C*) Estimates of PrP^{Sc} concentrations ($n = 3$ mice) in the cortex (*B*) and thalamus (*C*) are given. Relative PrP^{Sc} levels from infected DMSO mice at 78, 85, 92, and 99 dpi were estimated by using data from an earlier study.

toward secretory function at the expense of absorptive function (16, 28, 29). Whether Qa-induced cardiac abnormalities or GSI-induced malnutrition were the immediate causes of death is being investigated.

Sustained Suppression of PrP^{Sc} Levels. Because both the dose and the duration of GSI treatment contribute to adverse side effects, we examined the effect of a shorter exposure to 5 $mg \cdot kg^{-1} \cdot d^{-1}$ GSI and Qa. We began administration of 5 $mg \cdot kg^{-1} \cdot d^{-1}$ GSI plus 40 $mg \cdot kg^{-1} \cdot d^{-1}$ Qa to 15 mice at 50 dpi but reduced the duration from 43 to 28 d. The RML-infected mice were killed at 50, 78, 85, 92, 99, and 106 dpi, and PrP^{Sc} levels were measured by Western blots that were quantified by densitometry (Fig. 4). As controls, PrP^{Sc} levels were measured in age-matched, RML-infected, DMSO mice killed at 50 and 106 dpi. The relative PrP^{Sc} levels for the intermediate time points for untreated, RML-infected controls were inferred based on the PrP^{Sc} levels from an earlier study (6).

In the mice treated with GSI plus Qa for 28 d, PrP^{Sc} in the cortex was undetectable until 99 dpi (Fig. 4 *A* and *B*). In addition, although the level of PrP^{Sc} at 106 dpi was far below that in the untreated, control DMSO mice, there was a rapid increase in PrP^{Sc} in the thalamus between 99 and 106 dpi (Fig. 4 *A* and *C*), accompanied by a similar, although less dramatic, rise in PrP^{Sc} in the cortex (Fig. 4*B*). We do not know, however, whether the PrP^{Sc} in the two groups becomes similar by ≈120 d, when the RML-infected, control DMSO mice develop signs of neurological dysfunction. It was encouraging that the mice that received GSI plus Qa for 28 d exhibited normal behavior and normal brain and body weights. The mice also showed no hair loss. The successful suppression of PrP^{Sc} in some regions of the brain by GSI plus Qa suggests that it might be possible to develop effective treatment schedules based on intermittent administration of antiprion pharmacotherapeutics.

Discussion

In the studies reported here, we were able to manipulate pharmacologically the levels of PrP^{Sc} and the accompanying dendritic atrophy in the brains of mice by using a combination of GSI and Qa. The mechanisms by which these two compounds act alone or together are unknown. We initially decided to explore the use of GSIs in altering the pathogenesis of prion disease after discovering that both PrP^{Sc} and NICD rise concurrently throughout the incubation period (4). Those results suggested that the increase in NICD might be responsible for dendritic atrophy and loss. The results reported here show that dendritic atrophy and loss occur at both low and high NICD levels (Figs. 2 and 3).

In contrast to GSI alone, GSI in combination with Qa prevented dendritic atrophy and loss. Dissecting the mechanism by which GSI

plus Qa prevents dendritic atrophy and loss is likely to be complicated (4, 30, 31). In addition to Notch-1, >26 different proteins are γ-secretase substrates, some of which yield signaling peptides when cleaved (32), such as ErbB-4, which stimulates dendrite growth (33, 34). Exploring the effects of Qa on γ-secretase activity will be of interest to probe the possibility that Qa might raise the levels of one or more growth factors that preserve dendrites or alter the ratio of inhibitory to stimulatory factors for dendrites.

We began by administering GSIs to prion-infected mice midway through the incubation period. In this study, 10 $mg{\cdot}kg^{-1}{\cdot}d^{-1}$ LY411575 was tolerated poorly, but the 50% lower dose allowed us to give the drug for up to 43 d. Treatment with 5 $mg{\cdot}kg^{-1}{\cdot}d^{-1}$ GSI alone increased the level of PrP^{Sc} in the thalamus, had no effect on the level in hippocampus (Fig. 1*C*), but decreased the level of PrP^{Sc} in the cortex by nearly 50% (Fig. 1*A*). Although this finding suggested that GSI either selectively inhibited PrP^{Sc} formation or stimulated PrP^{Sc} clearance in the cortex, GSI more likely interfered with PrP^{Sc} transport from the thalamus to the cortex. In earlier studies, we and others demonstrated the initial replication of prions at the site of injection with transport along axons (35, 36). In the studies described here, PrP^{Sc} formation was initiated by intrathalamic inoculation of prions, and presumably anterograde axonal transport of PrP^{Sc} occurred along the monosynaptic thalamocortical system of axons that connects the thalamus with the cortex (1, 6, 37).

After 28 d of oral administration of 5 $mg{\cdot}kg^{-1}{\cdot}d^{-1}$ GSI combined with Qa, PrP^{Sc} levels remained higher in the thalamus than those in the cortex. Earlier studies showed that some PrP^{Sc} is released from degenerating neurons and their processes into the extracellular space of the CNS, where it accumulates in perivascular, subpial, and subependymal spaces (38, 39), and is taken up by activated microglia and reactive astrocytes (5, 37). Additionally, histoblots indicate that a substantial portion of the residual thalamic PrP^{Sc} is located in large bundles of axons within or immediately adjacent to the thalamus (Fig. 1*G*). Despite only reducing thalamic PrP^{Sc} levels by ≈50%, GSI plus Qa maintained dendrite loads to control levels, raising the possibility that PrP^{Sc} was either cleared from neurons but remained in the extracellular space or phagocytosed by glial cells, where it did not cause dendritic atrophy and loss.

From studies of Qa in cultured ScN2a cells, it appears that Qa inhibits the conversion of PrP^{C} into PrP^{Sc}. Studies with Qa attached to beads suggest that Qa binds preferentially to PrP^{Sc} (40). As shown in Fig. 1, 40 $mg{\cdot}kg^{-1}{\cdot}d^{-1}$ Qa reduced PrP^{Sc} levels minimally in the cortex and thalamus of CD1 mice but not the hippocampus. The addition of 5 $mg{\cdot}kg^{-1}{\cdot}d^{-1}$ GSI produced a 95% decrease in PrP^{Sc} levels of in cortex and hippocampus but only a 50% decline in the thalamus. The effect of Qa plus GSI was much greater than the sum of the two, demonstrating the synergistic reduction in PrP^{Sc}. Interestingly, the use of pentosan polysulfate (PPS) combined with iron(III) *meso*-tetra(4-sulfonatophenyl)porphine (FeTAP) produced a synergistic prolongation of incubation times in prion-infected mice (8). Although the combination of PPS and FeTAP had to be administered intracerebrally to effect a prolongation of the incubation period, the oral administration of 4-pyridinecarboxaldehyde-2-[4-(5-oxazolyl)phenyl]hydrazone (cpd-B) produced a doubling of the incubation time in RML-infected Tga20 mice when started midway through the incubation period (41).

Cpd-B was the most effective in prolonging the incubation times of RML-infected mice but had little effect on the incubation times of either Syrian hamsters or Tg(SHaPrP)7 mice inoculated intracerebrally with 263K prions (41). Combining cpd-B with a GSI will be of interest in the continuing search for an effective therapeutic regimen for CJD. Although the mechanism of action of cpd-B is unclear, learning how this compound diminishes the levels of PrP^{Sc} in cultured cells and brains of RML-infected mice will be important. Whether such a prion strain-specific pharmacotherapeutic can be adapted for the treatment of CJD is unknown. Low intermittent doses of a GSI might prove useful especially if one was found to act synergistically with a therapeutic agent such as cpd-B, which appears to be substantially more efficacious than Qa.

Despite the lack of success in identifying an effective therapy for CJD, the strategy of developing compounds that reduce PrP^{Sc} levels in cultured cells and the brains of rodents continues to seem reasonable. Disruption of the PrP gene prevents PrP^{Sc} formation and illness in mice (42, 43). Moreover, ≈95% suppression of PrP^{C} expression in mice harboring an inducible PrP transgene delays the onset of neurological dysfunction, resulting in incubation times that exceed 400 d (44). The discovery of protease-sensitive forms of PrP^{Sc} ($sPrP^{Sc}$) that can cause pathological changes in the CNS has brought a new dimension to the study of therapeutics (45–49). Future investigations will need to measure both $sPrP^{Sc}$ and protease-resistant PrP^{Sc} in response to therapeutics designed to treat the prion diseases (50).

Materials and Methods

Animals and Diet. Male CD1 mice were inoculated at 7 weeks of age with 30 μl of either RML prions (51) or a 10% brain homogenate from uninfected CD1 mice. Inocula were injected directly into the right thalamus.

The chocolate-flavored mouse liquid diet was prepared by adding water and cocoa powder (Hershey) to a commercially available liquid rat diet, LD'82 (Bio-Serv Inc.). LY411575 was prepared in the Chemical Synthesis Core at the Mayo Clinic according to the method of Fauq *et al.* (52) and solubilized in DMSO (Sigma–Aldrich) in a stock solution of 100 mg/ml. The final concentration of DMSO in GSI-containing drink was 0.007%. Qa was obtained from Sigma. Drugs were mixed with the liquid diet. To deliver 40 $mg{\cdot}kg^{-1}{\cdot}d^{-1}$ Qa per mouse, 900 g of LD'82 was mixed with 4 liters of water, 50 g of cocoa, and 0.315 g of Qa. DMSO also was added to the chocolate drink with Qa alone to a final concentration of 0.007%. The mice were fed ad libitum. Mice not receiving treatment were given chocolate drink with 0.007% DMSO.

Treatment and Diagnosis. Treated animals were fed chocolate drink, prepared with the drugs as described above. Untreated, control mice were given chocolate drink with DMSO alone unless otherwise specified. Groups of nine mice received either DMSO alone, Qa alone at 40 $mg{\cdot}kg^{-1}{\cdot}d^{-1}$, GSI alone at 5 $mg{\cdot}kg^{-1}{\cdot}d^{-1}$, or a combination of GSI and Qa at the doses specified. One group of uninfected control mice and RML-infected mice also were given GSI at 10 $mg{\cdot}kg^{-1}{\cdot}d^{-1}$. Treatment was initiated at 50 dpi and continued for 43 d (Figs. 1–3) or 28 d (Fig. 4).

Mice were monitored twice a week for neurological signs by observing their gait, mobility, posture, clasping reflex, righting reflex, behavior, and body condition. After onset of signs, they were monitored daily. Euthanasia was performed if two or more of the following neurological signs were present: mild ataxia, slight head tremors, head tilt, tail rigidity, dysmetria, clasping, or circling.

Tissue Dissection, Fixation, and Analysis. These methods are described in the *SI Text*.

ACKNOWLEDGMENTS. We thank the staff at the Hunter's Point animal facility, and we thank Ms. Hang Nguyen and Bernadette DeArmond, MD, MPH, for editing the manuscript. This work was funded by National Institutes of Health Grants AG10770, AG02132, AG25531, and AG021601 and by the Stephen and Patricia Schott Family Fund.

1. Bouzamondo-Bernstein E, *et al.* (2004) The neurodegeneration sequence in prion diseases: Evidence from functional, morphological and ultrastructural studies of the GABAergic system. *J Neuropathol Exp Neurol* 63:882–899.
2. Cox DL, Sing RR, Yang S (2006) Prion disease: Exponential growth requires membrane binding. *Biophys J* 90:L77–L79.
3. Hecker R, *et al.* (1992) Replication of distinct scrapie prion isolates is region specific in brains of transgenic mice and hamsters. *Genes Dev* 6:1213–1228.
4. Ishikura N, *et al.* (2005) Notch-1 activation and dendritic atrophy in prion disease. *Proc Natl Acad Sci USA* 102:886–891.
5. Mallucci G, *et al.* (2003) Depleting neuronal PrP in prion infection prevents disease and reverses spongiosis. *Science* 302:871–874.

6. Tatzelt J, Groth DF, Torchia M, Prusiner SB, DeArmond SJ (1999) Kinetics of prion protein accumulation in the CNS of mice with experimental scrapie. *J Neuropathol Exp Neurol* 58:1244–1249.
7. Trevitt CR, Collinge J (2006) A systematic review of prion therapeutics in experimental models. *Brain* 129:2241–2265.
8. Kocisko DA, Caughey B, Morrey JD, Race RE (2006) Enhanced antiscrapie effect using combination drug treatment. *Antimicrob Agents Chemother* 50:3447–3449.
9. Wisniewski T, Sigurdsson EM (2007) Therapeutic approaches for prion and Alzheimer's diseases. *FEBS J* 274:3784–3798.
10. Jeffrey M, *et al.* (2000) Synapse loss associated with abnormal PrP precedes neuronal degeneration in the scrapie-infected murine hippocampus. *Neuropathol Appl Neurobiol* 26:41–54.
11. De Strooper B, *et al.* (1999) A presenilin-1-dependent γ-secretase-like protease mediates release of Notch intracellular domain. *Nature* 398:518–522.
12. Mumm JS, Kopan R (2000) Notch signaling: From the outside in. *Dev Biol* 228:151–165.
13. Okochi M, *et al.* (2002) Presenilins mediate a dual intramembranous γ-secretase cleavage of Notch-1. *EMBO J* 21:5408–5416.
14. Allen T, Lobe CG (1999) A comparison of Notch, Hes and Grg expression during murine embryonic and post-natal development. *Cell Mol Biol (Noisy-le-grand)* 45:687–708.
15. Kageyama R, Ohtsuka T (1999) The Notch-Hes pathway in mammalian neural development. *Cell Res* 9:179–188.
16. Wong GT, *et al.* (2004) Chronic treatment with the γ-secretase inhibitor LY-411,575 inhibits β-amyloid peptide production and alters lymphopoiesis and intestinal cell differentiation. *J Biol Chem* 279:12876–12882.
17. Minter LM, *et al.* (2005) Inhibitors of γ-secretase block in vivo and in vitro T helper type 1 polarization by preventing Notch upregulation of Tbx21. *Nat Immunol* 6:680–688.
18. Doh-ura K, Iwaki T, Caughey B (2000) Lysosomotropic agents and cysteine protease inhibitors inhibit scrapie-associated prion protein accumulation. *J Virol* 74:4894–4897.
19. Korth C, May BCH, Cohen FE, Prusiner SB (2001) Acridine and phenothiazine derivatives as pharmacotherapeutics for prion disease. *Proc Natl Acad Sci USA* 98:9836–9841.
20. Collins SJ, *et al.* (2002) Quinacrine does not prolong survival in a murine Creutzfeldt–Jakob disease model. *Ann Neurol* 52:503–506.
21. Barret A, *et al.* (2003) Evaluation of quinacrine treatment for prion diseases. *J Virol* 77:8462–8469.
22. Huang Y, *et al.* (2006) Quinacrine is mainly metabolized to mono-desethyl quinacrine by CYP3A4/5 and its brain accumulation is limited by P-glycoprotein. *Drug Metab Dispos* 34:1136–1144.
23. Shaked GM, Engelstein R, Avraham I, Kahana E, Gabizon R (2003) Dimethyl sulfoxide delays PrP^{Sc} accumulation and disease symptoms in prion-infected hamsters. *Brain Res* 983:137–143.
24. Yung L, *et al.* (2004) Pharmacokinetics of quinacrine in the treatment of prion disease. *BMC Infect Dis* 4:53–59.
25. Barten DM, Meredith JE, Jr, Zaczek R, Houston JG, Albright CF (2006) γ-Secretase inhibitors for Alzheimer's disease: Balancing efficacy and toxicity. *Drugs R&D* 7:87–97.
26. Goodman LS, Gilman A (1955) *The Pharmacological Basis of Therapeutics* (Macmillan, New York).
27. Wallace DJ (2002) in *Dubois' Lupus Erythematosis*, eds Wallace DJ, Hahn BH (Lippincott, Philadelphia), pp 1149–1172.
28. Milano J, *et al.* (2004) Modulation of notch processing by γ-secretase inhibitors causes intestinal goblet cell metaplasia and induction of genes known to specify gut secretory lineage differentiation. *Toxicol Sci* 82:341–358.
29. van Es JH, *et al.* (2005) Notch/γ-secretase inhibition turns proliferative cells in intestinal crypts and adenomas into goblet cells. *Nature* 435:959–963.
30. Redmond L, Ghosh A (2001) The role of Notch and Rho GTPase signaling in the control of dendritic development. *Curr Opin Neurobiol* 11:111–117.
31. Sestan N, Artavanis-Tsakonas S, Rakic P (1999) Contact-dependent inhibition of cortical neurite growth mediated by notch signaling. *Science* 286:741–746.
32. Parks AL, Curtis D (2007) Presenilin diversifies its portfolio. *Trends Genet* 23:140–150.
33. Goldsmit Y, Erlich S, Pinkas-Kramarski R (2001) Neuregulin induces sustained reactive oxygen species generation to mediate neuronal differentiation. *Cell Mol Neurobiol* 21:753–769.
34. Vaskovsky A, Lupowitz Z, Erlich S, Pinkas-Kramarski R (2000) ErbB-4 activation promotes neurite outgrowth in PC12 cells. *J Neurochem* 74:979–987.
35. Taraboulos A, *et al.* (1992) Regional mapping of prion proteins in brains. *Proc Natl Acad Sci USA* 89:7620–7624.
36. Brandner S, *et al.* (1996) Normal host prion protein necessary for scrapie-induced neurotoxicity. *Nature* 379:339–343.
37. Kovacs GG, Preusser M, Strohschneider M, Budka H (2005) Subcellular localization of disease-associated prion protein in the human brain. *Am J Pathol* 166:287–294.
38. DeArmond SJ, *et al.* (1985) Identification of prion amyloid filaments in scrapie-infected brain. *Cell* 41:221–235.
39. DeArmond SJ, *et al.* (1987) Changes in the localization of brain prion proteins during scrapie infection. *Neurology* 37:1271–1280.
40. Phuan P-W, *et al.* (2007) Discriminating between cellular and misfolded prion protein by using affinity to 9-aminoacridine compounds. *J Gen Virol* 88:1392–1401.
41. Kawasaki Y, *et al.* (2007) Orally administered amyloidophilic compound is effective in prolonging the incubation periods of animals cerebrally infected with prion diseases in a prion strain-dependent manner. *J Virol* 81:12889–12898.
42. Büeler H, *et al.* (1993) Mice devoid of PrP are resistant to scrapie. *Cell* 73:1339–1347.
43. Prusiner SB, *et al.* (1993) Ablation of the prion protein (PrP) gene in mice prevents scrapie and facilitates production of anti-PrP antibodies. *Proc Natl Acad Sci USA* 90:10608–10612.
44. Safar JG, *et al.* (2005) Prion clearance in bigenic mice. *J Gen Virol* 86:2913–2923.
45. Safar J, *et al.* (1998) Eight prion strains have PrP^{Sc} molecules with different conformations. *Nat Med* 4:1157–1165.
46. Tzaban S, *et al.* (2002) Protease-sensitive scrapie prion protein in aggregates of heterogeneous sizes. *Biochemistry* 41:12868–12875.
47. Tremblay P, *et al.* (2004) Mutant PrP^{Sc} conformers induced by a synthetic peptide and several prion strains. *J Virol* 78:2088–2099.
48. Safar JG, *et al.* (2005) Diagnosis of human prion disease. *Proc Natl Acad Sci USA* 102:3501–3506.
49. Pastrana MA, *et al.* (2006) Isolation and characterization of a proteinase K-sensitive PrP^{Sc} fraction. *Biochemistry* 45:15710–15717.
50. Colby DW, *et al.* (2007) Prion detection by an amyloid seeding assay. *Proc Natl Acad Sci USA* 104:20914–20919.
51. Chandler RL (1962) Encephalopathy in mice. *Lancet* 279:107–108.
52. Fauq AH, Simpson K, Maharvi GM, Golde T, Das P (2007) A multigram chemical synthesis of the γ-secretase inhibitor LY411575 and its diastereoisomers. *Bioorg Med Chem Lett* 17:6392–6395.